

## Casimir force in a critical film formed from an electrolytic solution

A. Mukhopadhyay and B. M. Law

Condensed Matter Laboratory, Department of Physics, Kansas State University, Manhattan, Kansas 66506-2601

(Received 13 September 2000; published 29 March 2001)

We have studied the thickness of vapor adsorbed films of the critical binary liquid mixture acetic acid plus nonane adsorbed onto a silicon wafer substrate as a function of temperature near the critical temperature. This critical film possesses opposite boundary conditions (+ -) at its two surfaces and, due to the dissociation of acetic acid, both the electrostatic force and the dispersion force affect the adsorbed film thickness. On approaching the critical temperature  $T_c$ , an increase in the film thickness  $L$  is observed, implying that the sign of the universal Casimir amplitude  $\Delta^{+-}$  is positive, consistent with theoretical predictions. However, we find quantitative discrepancies in the value of  $\Delta^{+-}$  and the form of the critical Casimir pressure scaling function  $\vartheta^{+-}$  compared with previous experimental results. We attribute these discrepancies to the complex nature of the critical system studied in this experiment.

DOI: 10.1103/PhysRevE.63.041605

PACS number(s): 68.35.Rh, 68.35.Md, 64.60.Fr, 68.15.+e

### I. INTRODUCTION

Finite-size scaling within thin *critical* films has been used for many years to extrapolate the results of finite-size simulations to larger systems [1], however, it has only been in the last couple of years that experimentalists have directly examined the consequences of critical fluctuations within finite-sized films [2,3]. Within critical films of an *AB* binary liquid mixture, preferential adsorption of one of the components occurs at each surface thus giving rise to a variation in the composition as a function of depth into the film [4,5]. The composition profile, on each surface, has a width described by the bulk correlation length  $\xi = \xi_0 t^{-\nu}$  where  $\xi_0$  is the correlation length amplitude,  $\nu$  ( $=0.634$ ) is a bulk critical exponent, and  $t = |T - T_c|/T_c$  is the reduced temperature. Near a continuous or second-order phase transition  $\xi$  diverges. When  $\xi$  becomes of the order of the film thickness  $L$  the adsorption profile at one surface is distorted by the presence of the other surface; this generates a force between the boundaries [6], called the critical Casimir force, which exists over and above any noncritical dispersion and/or electrostatic forces that may be present. Theoretical results predict that the Casimir force in a critical film is governed by a universal Casimir pressure scaling function  $\vartheta(y)$  which depends only upon the ratio  $y = L/\xi$  [7]. At the critical point, the correlation length  $\xi \rightarrow \infty$ , therefore  $y = 0$  and the scaling function  $\vartheta(0)/2$  defines a universal amplitude  $\Delta$  known as the Casimir amplitude. The form of the scaling function  $\vartheta(y)$  and the value of the Casimir amplitude  $\Delta$  depend upon the system universality class (i.e., Ising, *XY*, etc.) and the boundary conditions at the two surfaces of the film. Experimental evidence for the existence of a critical Casimir force in thin adsorbed films has been reported for binary liquid mixtures near their demixing transition [2] and for  $^4\text{He}$  near the superfluid transition [3]. In this paper we use the experimental technique of ellipsometry to study finite-size effects in the system acetic acid plus nonane (AN) adsorbed onto a silicon wafer substrate. In previous systems, studied by our group, both the dispersion force and the critical Casimir force were present. For the mixture AN, acetic acid dissociates in solution, which gives rise to an additional electrostatic force.

Hence this paper compares finite-size effects within a thin adsorbed *ionic* film (specifically AN) to previous results [2,8] within *nonionic* films.

The plan of this paper is as follows. In Sec. II we discuss factors that determine the equilibrium thickness of the adsorbed film. The experimental configuration and the experimental technique of ellipsometry are described in Sec. III. In Sec. IV we report on and discuss the experimental results.

### II. FREE-ENERGY CONSIDERATIONS

If a molecularly smooth and homogeneous surface is suspended above a critical binary liquid mixture as depicted in Fig. 1, a thin adsorbed film of the liquid mixture will form on this solid surface. At a height  $H$  above the liquid mixture many factors determine the thickness of this adsorbed film.

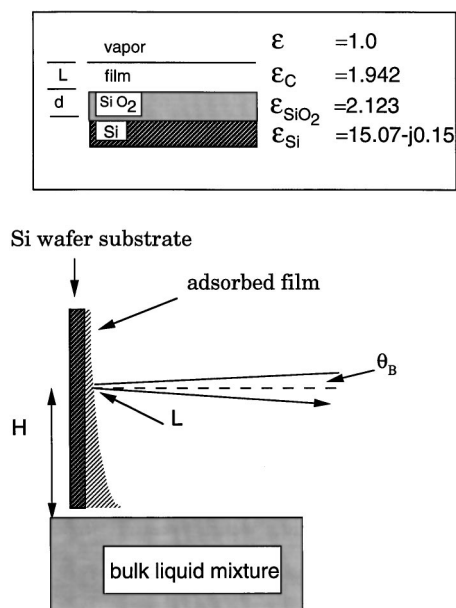


FIG. 1. Schematic diagram showing the vertical Si wafer substrate geometry. The inset depicts the dielectric model used to obtain the adsorption film thickness  $L$  for films on an oxide coated Si wafer.

For nonionic fluids *far* from the critical temperature ( $T_c$ ) the equilibrium film thickness is determined by a competition between gravity (which thins the layer) and the dispersion force (which thickens the layer) [9]. Assuming that both surfaces of the film are sharp and that the capillary-wave fluctuations at the film's liquid-vapor surface are small, the equilibrium film thickness  $L(H)$  is given by

$$F(L) + \rho g H = 0, \quad (1)$$

where  $\rho$  is the density of the liquid and  $g$  is the acceleration due to gravity.  $F(L)$  is the dispersion force per unit area on each of the two semi-infinite phases, the solid substrate and the vapor, when they are separated by a gap of width  $L$  occupied by the liquid film.

For sufficiently thin films ( $L \leq 10-20$  nm), in the nonretarded regime,  $F(L)$  can be written in the form [10]

$$F(L) = -2W(T)/L^3, \quad (2)$$

where  $W(T)$  is the system dependent Hamaker constant. The Dzyaloshinskii, Lifshitz, and Pitaevskii (DLP) theory [11] for dispersion forces provides a more general expression for  $F(L)$ , valid at all thicknesses  $L$ . It includes both the nonadditivity of the intermolecular forces and retardation effects and can be used to provide an expression for  $W$  in terms of the absorption spectra of the bulk phases. Equations (1) and (2) together imply that at a particular height  $H$ , the equilibrium thickness of the adsorbed film can be written as

$$L = \left( \frac{2W}{\rho g H} \right)^{1/3}. \quad (3)$$

A film only forms provided that the Hamaker constant possesses the correct sign, namely,  $W > 0$  in Eq. (3). This condition is satisfied automatically for most organic liquids on a Si wafer due to the large optical dielectric constant for silicon ( $\epsilon_{\text{Si}} \sim 15$ ).

On solid substrates the prediction that  $L \sim H^{-1/3}$  found confirmation in low-temperature experiments [12] where for thicker films the more general DLP theory for  $F(L)$  had to be used. For film thicknesses, which are of the order of a few times the molecular diameter, the continuum theory for the dispersion interaction breaks down and the oscillatory solvation force within the adsorbed film becomes important [13]. To account for a solvation force, a monotonic repulsive structural interaction term must be included in Eq. (1). The equilibrium thickness of the adsorbed film at a height  $H$  is then determined by

$$\frac{2W}{L^3} - \frac{A \exp(-L/\delta)}{\delta} = \rho g H, \quad (4)$$

where  $\delta$  is of order a molecular diameter. Far above the critical temperature, adsorbed films formed from the binary liquid mixtures methanol plus hexane (MH) and 2-methoxyethanol plus methylcyclohexane (MM) against a Si wafer are well described by Eq. (4), although the experimentally determined values for the Hamaker constant do not agree with the calculated value using the DLP theory [2].

This discrepancy for the Hamaker constant was attributed to the fact that the adsorbed films, in these experiments, formed in the partial wetting regime of the substrate as indicated by contact angle measurements. Equations (3) and (4) assume complete wetting of the substrate by the adsorbed film [8].

The dispersion force and the structural force determine the substrate-film interaction strictly for systems involving nonionic wetting films on uncharged surfaces. More complex effects can occur within these thin adsorbed films if, for example, either the substrate is ionizable or the film possesses ions in solution. For surfaces that undergo surface dissociation when in contact with a liquid or a thin film, the surface becomes charged and the counterions in solution form a diffuse double layer in the vicinity of the interface which is described by the Poisson-Boltzmann equation [10]. If, in addition, a dissolved salt or ions are present within the thin film then this may regulate the surface charge and the distribution of counterions. Kayser has considered these questions in depth for a binary liquid film in contact with an ionizable surface with [14] and without [15] a salt present. It is assumed in [14,15] that adsorption is absent, namely, the  $A$  and  $B$  molecules are randomly distributed throughout the thin film, and that the charged surface only influences the distribution of counterions and dissolved salt ions. Kayser's most general expressions are very complicated with many parameters that are difficult to measure or estimate, however, for thick films or high surface charge densities his expressions reduce to a simple Langmuir model [16] which accounts for electrical double layer effects

$$L = (k_B T / z e) (\pi^2 \epsilon \epsilon_0 / 2 \rho g H)^{1/2}, \quad (5)$$

where  $z$  is the ionic valence,  $\epsilon$  is the static dielectric constant of the liquid, and all other symbols have their usual meaning. The electrostatic force due to the electrical double layer possesses a much longer range [as indicated by  $L \sim H^{-1/2}$  in Eq. (5)] compared with the nonretarded dispersion force [where  $L \sim H^{-1/3}$ , Eq. (3)].

For the mixture of interest, AN, acetic acid ( $\text{CH}_3\text{COOH}$ ) dissociates in the solvent to form  $\text{CH}_3\text{COO}^-$  and  $\text{H}^+$  ions, where the relative concentration of neutral molecules to the ions is determined by the dissociation constant for the reaction



in the solvent nonane. Ions are certainly present in the bulk mixture where the  $\text{pH} \sim 2$ ; they are expected to be present also in the thin adsorbed film. However, the precise conditions within the thin adsorbed film are not known, therefore, rather than using Kayser's more general expressions we will represent the presence of an electrical double layer by a term similar to Langmuir's result [Eq. (5)] for simplicity. For temperatures far from the critical temperature we assume that the equilibrium condition that includes the effects of dispersion, ionic and structural forces can be written as

$$\frac{C(T)}{L^2} + \frac{2W(T)}{L^3} - \frac{A \exp(-L/\delta)}{\delta} = \rho g H, \quad (7)$$

where  $C(T)$  is a constant that depends upon the ionic properties of the substrate and the solvent [14]. Since both  $C$  and  $W$  depend only weakly on the absolute temperature  $T$ , over the small temperature range that we consider here, their temperature dependence can be neglected.

Close to the critical temperature  $T_c$ , concentration fluctuations within the film give rise to an additional critical Casimir pressure between the film boundaries. This critical Casimir pressure  $p_c$  is given by [7]

$$p_c = \frac{k_B T_c}{L^3} \vartheta^{ab} \left( \frac{L}{\xi} \right), \quad (8)$$

where the universal surface scaling function  $\vartheta^{ab}(y)$  is related to the universal Casimir amplitude  $\Delta^{ab}$  by the relation  $\vartheta^{ab}(0) = 2\Delta^{ab}$ . The superscript  $ab$  specifies the surface universality classes on the two confining boundaries of the film. In the limit of a strong surface field, which is expected under normal conditions sufficiently close to  $T_c$ , one of the components exhibits complete saturation against each boundary. For this situation there are only two different combinations of boundary conditions  $ab$  that need to be considered for a film of a binary liquid mixture; similar boundary conditions  $(++)$ , where the same component preferentially adsorbs at both surfaces, and opposite boundary conditions  $(+-)$ , where different components adsorb at the two surfaces. The Casimir force in a critical film is predicted to depend crucially upon the boundary conditions at the surfaces of this film.

For a critical film on a Si wafer substrate one boundary of the film is the Si wafer, while the other boundary is the free liquid-vapor surface. For AN, nonane adsorbs at the liquid-vapor surface (as it possesses the lower surface tension) while acetic acid adsorbs at the liquid-substrate surface (as was verified by noting that the liquid-liquid meniscus against the Si wafer bends away from the acetic acid rich phase in the two-phase region of the liquid mixture). This mixture therefore constitutes an experimental realization of the  $+ -$  boundary condition. For more details about the effect of the critical Casimir force on a binary liquid film, and relevant theoretical considerations, see Ref. [8].

Finally, combining Eqs. (7) and (8) we obtain the principal equation, which controls the thickness of the adsorbed film near  $T_c$ ,

$$\frac{C}{L^2} + \frac{2W}{L^3} - \frac{A \exp(-L/\delta)}{\delta} + \frac{k_B T_c}{L^3} \vartheta^{ab} \left( \frac{L}{\xi} \right) = \rho g H. \quad (9)$$

One can extract the functional form of the surface scaling function  $\vartheta^{ab}$  from this equation by experimentally measuring the adsorbed film thickness as a function of temperature near the bulk critical temperature [17]. Ellipsometry can measure the average film thickness very accurately with a resolution of  $\sim 0.001$  nm on a Si wafer substrate. In this paper we use this technique to deduce the function  $\vartheta^{+-}$  for the critical ionic mixture AN in order to compare it with our previous determination from critical nonionic systems [2].

### III. EXPERIMENTAL TECHNIQUE

A phase modulated ellipsometer was used to measure the thickness of the vapor-adsorbed film on the substrate [18]. The Si wafer was suspended vertically above the liquid mixture inside a cylindrical glass cell where a metal clip mechanically held the wafer against a chemically resistant stainless-steel plate. The temperature of the sample cell is controlled by a two stage thermostat constructed from concentric metallic shells which are thermally isolated from each other. These two stages possess a combined thermal stability of  $\sim 0.1$  mK over 2 h and  $\sim 1$  mK over a day, as measured by two matched precision thermistors (Yellow Spring Instruments, Catalog No. 44034) placed at either end of the sample cell. A He-Ne laser beam from the ellipsometer, which is focused to a small spot ( $\sim 0.25$  mm), is reflected off the Si wafer at a height  $H$  above the liquid-vapor surface at an angle of incidence equal to the Brewster angle,  $\theta_B$  ( $\sim 75.53^\circ$ ), for the bare Si wafer. The signal measured by the ellipsometer  $\bar{\rho}$ , is very sensitive to the surface structure at this angle of incidence and can be readily interpreted in terms of the film thickness [19]. The extreme sensitivity of ellipsometry and its application in measurements of both the optical constants and the thickness of thin liquid films are well documented in the literature [20].

The ellipticity,  $\bar{\rho} = \text{Im}(r_p/r_s)_{\theta_B}$ , measured by the ellipsometer is the imaginary component of the ratio of complex reflection amplitudes in the  $p$  and  $s$ -polarization directions at the Brewster angle. At this angle the Fresnel term vanishes, consequently,  $\text{Re}(r_p/r_s)_{\theta_B} = 0$  and this condition is used as an operational definition in determining the angle of incidence  $\theta_B$  [18]. In the absence of any capillary wave fluctuations,  $\bar{\rho}$  is related to the optical dielectric profile  $\epsilon(z)$  at depth  $z$  within the interface according to the Drude equation [21]

$$\bar{\rho} = \frac{\pi}{\lambda} \frac{\sqrt{\epsilon_1 + \epsilon_3}}{\epsilon_1 - \epsilon_3} \int \frac{[\epsilon(z) - \epsilon_1][\epsilon(z) - \epsilon_3]}{\epsilon(z)} dz. \quad (10)$$

Here  $\epsilon_1$  and  $\epsilon_3$  represent the optical dielectric constants of the incident ( $z \rightarrow -\infty$ ) and the substrate media ( $z \rightarrow \infty$ ), respectively. This formula assumes that  $\epsilon(z)$  is locally isotropic and that the thickness of the film is small compared with the wavelength of the incident light for which  $\lambda = 632.8$  nm.

A model for  $\epsilon(z)$  is required in order to determine the adsorbed film thickness  $L$  from the ellipsometric data. We assume that  $\epsilon(z) = \epsilon_c (= 1.942)$ ; the dielectric constant of the liquid film AN at the critical composition. Silicon wafers normally possess an oxide layer of thickness  $d$  ( $\sim$  nm) and optical dielectric constant  $\epsilon_{\text{SiO}_2} (= 2.123)$ . Therefore a reasonable model for the adsorbed film on the Si wafer is the two layer model exhibited in the inset to Fig. 1. With this model for  $d, L \ll \lambda$ , Eq. (10) implies that  $\bar{\rho}$  is proportional to the film thickness  $L$ ,

TABLE I. Critical liquid mixture properties.

$T_c$ (K)	$m_c^a$	$\epsilon_c^b$	$\xi_{o+}^c$ (nm)	$W=0$			$C=0$		
				$10^{15}C$ (N)	$A$ (J/m <sup>2</sup> )	$\delta$ (nm)	$10^{24}W$ (J)	$A$ (J/m <sup>2</sup> )	$\delta$ (nm)
311.95	0.605	1.942	0.39	0.8	$1.77 \times 10^{-4}$	0.33	2.70	$1.85 \times 10^{-4}$	0.33

<sup>a</sup>Critical mass fraction of acetic acid for AN.

<sup>b</sup>Optical dielectric constant at the critical composition for this mixture using data from [27].

<sup>c</sup>Correlation length amplitude in the one-phase region determined from critical adsorption measurements, as described in Ref. [23].

$$\bar{\rho} = \frac{\pi}{\lambda} \frac{\sqrt{1 + \epsilon_{\text{Si}}}}{1 - \epsilon_{\text{Si}}} \left[ \frac{(\epsilon_c - 1)(\epsilon_c - \epsilon_{\text{Si}})}{\epsilon_c} L + \frac{(\epsilon_{\text{SiO}_2} - 1)(\epsilon_{\text{SiO}_2} - \epsilon_{\text{Si}})}{\epsilon_{\text{SiO}_2}} d \right]. \quad (11)$$

Our bare Si wafer surfaces typically gave  $\bar{\rho} = 0.020 \pm 0.001$ , which from Eq. (11), corresponds to an oxide film thickness of  $d \sim 2.0$  nm. The large real component for the Si optical dielectric constant ( $\epsilon_{\text{Si}} \sim 15.07$ ) provides a strong dependence for the ellipticity  $\bar{\rho}$  upon the film thickness  $L$ . We measure  $\bar{\rho}$  with a sensitivity of  $\sim 10^{-5}$  corresponding to a thickness sensitivity of  $\sim 0.001$  nm averaged over the size of the incident beam spot for organic liquids on silicon.

In a typical ellipsometric measurement the temperature is set and approximately 8 h is allowed for the system to attain thermal and diffusive equilibrium. Twenty  $\bar{\rho}$  and  $T$  measurements are then collected over the next 2 h. From these 20 measurements the mean and standard deviation for  $\bar{\rho}$  are determined. The typical standard deviation of  $\bar{\rho}$  for each data point was  $\sim 3 \times 10^{-4}$ , however, different temperature scans on the same liquid exhibited a reproducibility for  $\bar{\rho}$  of  $\pm 3 \times 10^{-3}$ . We therefore took this later value (corresponding to an error in  $L$  of  $\sim \pm 0.3$  nm) as a conservative estimate for the error in  $\bar{\rho}$ .

The (100) Si wafers used in this experiment were purchased from Semiconductor Processing Company. They possessed a radius of 3.8 cm, thickness of 0.2 cm, and had been diced into quarters for ease of handling. They were polished on one side and possessed an *n*-type phosphorous doping with a resistivity of 1–10  $\Omega$ –cm. The polished surface of these wafers was carefully protected before diamond sawing to a Si substrate size of 3 cm  $\times$  1.5 cm. The Si substrate was carefully cleaned using the standard RCA Si wafer cleaning procedure [22] before mounting inside the cylindrical glass sample cell.

The organic liquids, acetic acid and nonane, used in this experiment had a quoted purity of 99% and 99.9%, respectively, and were purchased from Aldrich Chemical Company. The critical mass fraction  $m_c$  for this mixture (Table I) was determined using the standard procedure of observing the position of the liquid-liquid meniscus a few mK into the two-phase regime. At the critical composition the upper and

lower phases possess equal volume fractions and the meniscus is situated at the midpoint of the sample volume.

#### IV. EXPERIMENTAL RESULTS AND DISCUSSION

In Fig. 2 (and Table II) we show the adsorption thickness  $L$  as a function of  $\Delta T = T - T_c$  collected from a vertically oriented Si wafer at two different heights in the *one-phase* region for the critical mixture AN. The data are completely reproducible for both increasing and decreasing temperatures. As the temperature is reduced towards  $T_c$  the film thickness increases as a result of the critical Casimir force, which immediately indicates that both  $\Delta^{+-}$  and  $\vartheta^{+-}$  are positive, in agreement with theory. Before the surface scaling function  $\vartheta^{+-}(L/\xi)$  can be extracted all of the system dependent parameters  $W, C, A, \delta$ , and  $\xi$ , which appear in Eq. (9) must be determined. The correlation length amplitude  $\xi_0$  has been determined using critical adsorption ellipsometric measurements following the procedure in Ref. [23] (Table I). The parameters  $W, A, \delta$ , and  $C$  occur in the noncritical contributions to the force balance equation for the film; these terms, which are relatively temperature independent for the range of temperatures that we consider, are present at all temperatures both near to and far from  $T_c$ .  $W, A, \delta$ , and  $C$  can be determined by examining the variation of the adsorption thickness  $L$  with height  $H$  for fixed  $T \gg T_c$ . In Fig. 3 (and Table III) we show  $L$  versus  $H$  for the system AN at a

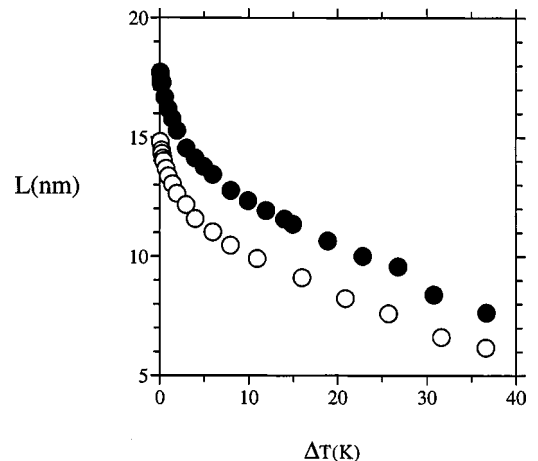


FIG. 2. Variation in the adsorption film thickness  $L$  as a function of  $\Delta T = T - T_c$  for the mixture AN at fixed height  $H = 1.5$  mm (solid circles) and  $H = 2.8$  mm (open circles).

TABLE II. One-phase data for AN.

$\Delta T(K)$	$L(nm)$	$\Delta T(K)$	$L(nm)$
$H=1.5$ mm			
36.69	7.65	3.99	14.13
30.76	8.41	3.00	14.54
26.77	9.57	1.94	15.28
22.81	10.02	1.40	15.79
18.89	10.66	0.94	16.20
14.96	11.36	0.56	16.69
14.00	11.58	0.29	17.29
11.97	11.94	0.15	17.41
9.95	12.35	0.14	17.28
7.98	12.77	0.06	17.73
5.98	13.45		
$H=2.8$ mm			
36.61	6.17	2.98	12.17
31.62	6.61	1.94	12.65
25.69	7.60	1.44	13.04
20.85	8.24	0.97	13.38
15.99	9.11	0.72	13.69
10.96	9.92	0.45	14.00
7.94	10.48	0.20	14.45
5.96	11.03	0.06	14.81
4.00	11.59		

temperature  $T=346$  K, which is  $\geq 30^{\circ}C$  above  $T_c$ , where the critical Casimir effect is expected to be small and  $\vartheta^{+-}$  can be neglected. The data exhibited in Fig. 3 can therefore be analyzed using Eq. (7). There are rather a large number (4) of adjustable parameters in Eq. (7). A reasonable approximation, which reduces the number of adjustable param-

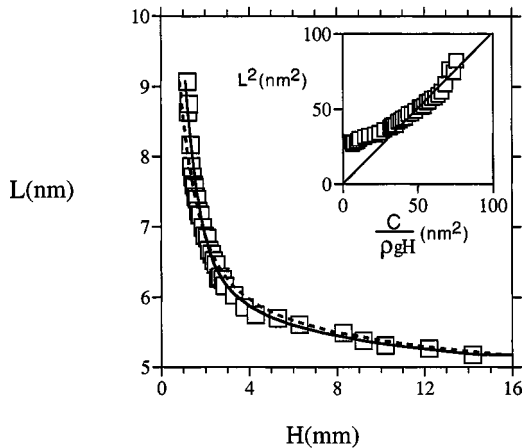


FIG. 3. Film thickness  $L$  as a function of height  $H$  for AN at a temperature of  $T=346$  K. The solid line is a fit to Eq. (12) (which assumes that  $W=0$ ) used in determining  $A$  and  $\delta$  as described in the text. The inset illustrates the  $L \sim H^{-1/2}$  dependence for small  $H$  (or large  $L$ ) from which the constant  $C$  is determined (where the solid line has a slope of 1). The dotted line, in the main figure, is a fit to Eq. (4) (which assumes that  $C=0$ ) used in determining the effective Hamaker constant  $W$  as described in the text.

TABLE III.  $L$  vs  $H$  data for the system AN at  $T=346$  K.

$H(mm)$	$L(nm)$	$H(mm)$	$L(nm)$
1.28	8.75	2.58	6.27
1.33	8.16	2.68	6.28
1.38	7.85	2.78	6.24
1.43	7.71	2.88	6.16
1.48	7.59	3.28	6.02
1.53	7.55	3.78	5.85
1.58	7.42	4.28	5.74
1.63	7.38	6.2	5.61
1.68	7.22	8.28	5.48
1.73	7.16	9.2	5.37
1.78	7.16	10.2	5.30
1.88	6.98	12.2	5.26
1.98	6.86	14.2	5.17
2.08	6.84	16.2	5.32
2.28	6.60		

eters, is to ignore the dispersion term, which is usually dominated by the ionic contribution [15], hence

$$\frac{C}{L^2} - \frac{A \exp(-L/\delta)}{\delta} = \rho g H. \quad (12)$$

For sufficiently large film thicknesses  $L$ , such that  $L/\delta \gg 1$ , the structural contribution is negligible and  $L \sim H^{-1/2}$  (Fig. 3 inset) from which the constant  $C$  can be estimated (Table I). At small  $L$  or large  $H$  the data in the Fig. 3 inset no longer follows a  $L \sim H^{-1/2}$  dependence; this indicates that the structural contribution in Eq. (12) is important in this regime. From Fig. 3, at sufficiently large  $H$  ( $\sim 12$  mm), the adsorption thickness  $L$  losses its dependence upon  $H$  and  $L$  approaches a constant value  $L^*$  ( $\approx 5.3$  nm); this implies that the gravitational term  $\rho g H$  in Eq. (12) does not play a major role in determining  $L^*$ . Instead  $L^*$  is determined by a competition between the electrostatic term and the structural term. Therefore, from Eq. (12),  $L^*$  is approximately related to  $C$ ,  $A$ , and  $\delta$  by the equation

$$\frac{C}{L^{*2}} = \frac{A \exp(-L^*/\delta)}{\delta}. \quad (13)$$

Equation (13) can be used to eliminate the parameter  $A$  from Eq. (12),

$$\frac{C}{L^2} - \frac{C}{L^{*2}} \exp[(L^* - L)/\delta] = \rho g H, \quad (14)$$

where only the parameter  $\delta$  is undetermined.  $\delta$  is adjusted to provide the best description of the crossover from  $L \sim H^{-1/2}$  to  $L=L^*$  behavior in Fig. 3 (solid line). The parameters  $C$ ,  $A$ , and  $\delta$  are listed in Table I for the system AN.

For comparison with the above analysis, where we assume that the ionic contribution dominates the dispersion contribution, we can consider the opposite extreme, namely,

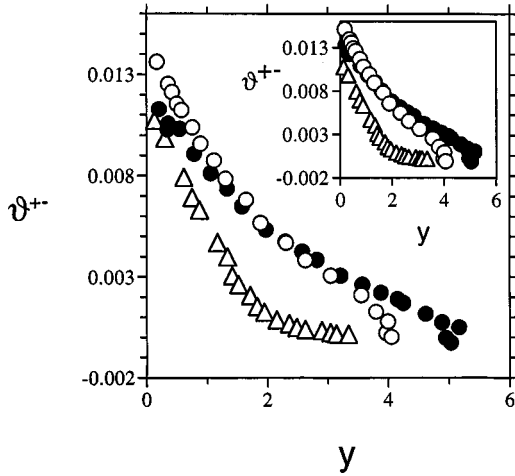


FIG. 4. The Casimir pressure scaling function  $\vartheta^{+-}(y)$  versus  $y=L/\xi$  for the mixture AN in the one-phase region where  $L$  is the film thickness and  $\xi$  is the correlation length. This graph was determined by substituting the data in Fig. 2 and the parameters from Table I (for  $W=0$ ) into Eq. (9). The symbols have the same meaning as in Fig. 2. In the inset we show the same function using Eq. (9) but for the parameters from Table I for  $C=0$ . For comparison we also show the surface scaling function for the nonionic critical mixture MH (triangles) from Ref. [2].

we neglect the ionic term ( $C=0$ ) and analyze the  $L$  versus  $H$  data far from  $T_c$  using Eq. (4). Such an analysis is strictly valid only for nonionic films. The authors used this method to determine  $W, A$ , and  $\delta$  for the nonionic binary liquid adsorbed films of MH and MM [8]. For the critical mixture AN, the dotted line in Fig. 3 is the best fit to the data using Eq. (4) with  $W, A$ , and  $\delta$  as adjustable parameters (Table I) [24]. As expected the previous analysis [which assumes the presence of an electrical double layer with  $C \neq 0$  and  $W=0$  (Fig. 3, solid line)] provides a (marginally) better description of the experimental data than the current method [which assumes a nonionic film with  $C=0$  and  $W \neq 0$  (Fig. 3, dotted line)].

With the system dependent parameters determined, the universal surface scaling function  $\vartheta^{+-}$  can be obtained using Eq. (9) by studying the adsorption thickness  $L$  as a function of  $T$  at fixed  $H$  (Fig. 2). Once again to simplify the complications, instead of using the full version of Eq. (9), we will consider the special cases when the dispersion term is neglected ( $W=0$ ) or when the electrostatic term is neglected ( $C=0$ ). In Fig. 4 (open and solid circles) we show the scaling function  $\vartheta^{+-}$  plotted against  $y=L/\xi$  for  $W=0$ , while in the inset, we show the same function for  $C=0$ . The system dependent parameters listed in Table I have been used in both cases. In contrast to the two critical systems MH and MM studied previously [2] the data does not collapse as well onto a single universal curve for AN, especially at small and large  $y$ . At  $y=0$ ,  $\vartheta^{+-}(0)=2\Delta^{+-}$  and therefore  $\Delta^{+-} \sim 0.0062$ , which is  $\sim 17\%$  larger than our previous determination of  $\Delta^{+-}$  [2]; however this value is still significantly smaller than theoretical expectations where  $\Delta^{+-} \sim 0.279$  to  $3.1$  [25]. On the same figure we also show the surface scaling function for the critical nonionic system MH (triangles)

where for clarity only a single height is plotted. For both models ( $W=0$  and  $C=0$ ) and for all values of  $y=L/\xi$ , the scaling function  $\vartheta^{+-}$  for AN lies above that of MH and possesses quite a different shape. This discrepancy cannot be due to the structural term in Eq. (9), which is only important for  $L \leq \delta$ . For the film thicknesses that are considered here, the contribution from the structural term to the surface scaling function is negligible.

For AN, the data collapse for the function  $\vartheta^{+-}$  when plotted against  $y=L/\xi$  is not as good as observed before for the systems MH and MM [2]. This may be due to our imperfect understanding of the noncritical part in the force balance equation for the film thickness. Obviously the system AN is complex in nature due to the dissociation of acetic acid in solution. This contributes an electrostatic term in the film free energy and a quantitative calculation of this term requires knowledge of the dissociation constant of the reaction (6) and the surface charge density of the  $\text{SiO}_2$  layer, which are difficult to determine for this system. A stringent analysis of the data should take into account both the dispersion term and the electrostatic term in fitting the  $L$  versus  $H$  data of Fig. 3 and then use those values of  $W$  and  $C$  in Eq. (9) to obtain the scaling function  $\vartheta^{+-}$ . Using this procedure for AN requires the determination of four adjustable parameters which considerably complicates the analysis. From Fig. 2, we note that the film thickness  $L$  for both heights still has quite a large temperature dependence even far away from  $T_c$ . This indicates that the critical Casimir force is still large at this temperature and the use of Eq. (7) to analyze the  $L$  versus  $H$  data may not be completely justified. However, various experimental constraints prevented us from acquiring measurements of the film thicknesses at any higher temperatures than given in this paper. Despite our reservations stated above concerning our analysis of the noncritical background contributions, the surface scaling function  $\vartheta^{+-}$  for the ionic mixture AN is considerably larger and possesses quite a different shape compared with the corresponding surface scaling function for nonionic mixtures as represented by MH in Fig. 4. This might be caused by our incomplete knowledge of the background contribution or it could be caused by the presence of a large electric field within the adsorbed film, associated with the electric double layer. It is well known that electric fields suppress critical fluctuations within critical mixtures and alter the position of the coexistence curve [26]. For the benefit of the reader, in case the noncritical free-energy contributions and/or the electric-field effects are better understood at some future date, we provide our film thickness data  $L$  as a function of  $\Delta T = T - T_c$  (at fixed  $H$ ) and of  $H$  (at fixed  $T$ ) in, respectively, Tables II and III.

In conclusion, in this paper we have studied the effect of the critical Casimir force on vapor-adsorbed films on molecularly smooth Si wafers suspended above a critical binary liquid mixture of AN. This system exhibits opposite (+ -) boundary conditions within the adsorbed film and, far from the critical temperature, both the van der Waals and the electrostatic force play roles in determining the adsorbed film thickness [Eq. (7)]. On approaching the critical temperature an increase in the adsorbed film thickness is observed (Fig. 2), implying that the sign of the critical Casimir pressure

scaling function  $\vartheta^{+-}$  and the universal Casimir amplitude  $\Delta^{+-}$  are positive. Both of these observations are in agreement with theoretical expectations and previous experimental observations. The value of  $\Delta^{+-}$  found in this experiment is  $\sim 17\%$  larger than an earlier determination for two (non-ionic) critical mixtures [2]. The function  $\vartheta^{+-}$  for AN does not scale as well when plotted against  $y=L/\xi$ ; it possesses quite a different shape and lies above the  $\vartheta^{+-}$  function determined for the nonionic mixture MH (Fig. 4). These dis-

crepancies may be due to our inadequate knowledge of the noncritical part of the film free energy for this system and/or they may be caused by the presence of a large electric field within the adsorbed film associated with the electric double layer.

This research was supported by the National Science Foundation through Grant No. DMR-9631133.

- 
- [1] *Finite Size Scaling and Numerical Simulations of Statistical Systems*, edited by V. Privman (World Scientific, Singapore, 1990).
- [2] A. Mukhopadhyay and B. M. Law, Phys. Rev. Lett. **83**, 772 (1999).
- [3] R. Garcia and M. H. W. Chan, Phys. Rev. Lett. **83**, 1187 (1999).
- [4] M. E. Fisher and P.-G. de Gennes, C. R. Seances Acad. Sci., Ser. B **287**, 207 (1978).
- [5] A. J. Liu and M. E. Fisher, Phys. Rev. A **40**, 7202 (1989).
- [6] M. Krech, *The Casimir Effect in Critical Systems* (World Scientific, Singapore, 1994), and references therein.
- [7] M. Krech and S. Dietrich, Phys. Rev. Lett. **66**, 345 (1991); **67**, 1055 (1991); Phys. Rev. A **46**, 1886 (1992).
- [8] A. Mukhopadhyay and B. M. Law, Phys. Rev. E **62**, 5201 (2000).
- [9] R. F. Kayser, Phys. Rev. B **34**, 3254 (1986).
- [10] J. N. Israelachvili, *Intermolecular and Surface Forces* (Academic, London, 1991), 2nd ed.
- [11] I. E. Dzyaloshinskii, E. M. Lifshitz, and L. P. Pitaevskii, Adv. Phys. **10**, 165 (1961).
- [12] E. S. Sabisky and C. H. Anderson, Phys. Rev. A **7**, 790 (1973); V. Panella, R. Chiarello, and J. Krim, Phys. Rev. Lett. **76**, 3606 (1996).
- [13] N. V. Churaev and B. V. Derjaguin, J. Colloid Interface Sci. **103**, 542 (1985).
- [14] R. F. Kayser, J. Phys. (France) **49**, 1027 (1988).
- [15] R. F. Kayser, Phys. Rev. Lett. **56**, 1831 (1986).
- [16] I. Langmuir, Science **88**, 430 (1938).
- [17] The temperature dependencies of  $C$  and  $W$  have been neglected in Eq. (9). They are not well understood; they will depend upon the absolute temperature  $T$  rather than the reduced temperature  $t$ . Perhaps, at most,  $C$  and  $W$  might exhibit a weak linear dependence upon  $T$ . In Ref. [2] we neglected any temperature dependence associated with  $W$  for nonionic films and found scaling for the function  $\vartheta^{+-}$  when plotted against  $y=L/\xi$ . *A posteriori* therefore the temperature dependence of  $W$  is indeed small otherwise scaling would not have been found.
- [18] D. Beaglehole, Physica B & C **100**, 163 (1980).
- [19] R. M. A. Azzam and N. M. Bashara, *Ellipsometry and Polarized Light* (North-Holland, Amsterdam, 1987).
- [20] D. Beaglehole, in *Fluid Interfacial Phenomena*, edited by C. A. Croxton (Wiley, New York, 1986).
- [21] P. Drude, *The Theory of Optics* (Dover, New York, 1959).
- [22] W. Kern and D. A. Puotinen, RCA Rev. **31**, 187 (1970).
- [23] J. H. Carpenter, B. M. Law, and D. S. P. Smith, Phys. Rev. E **59**, 5655 (1999).
- [24] The value of the Hamaker constant for the mixture AN on a Si wafer substrate listed in Table I ( $W=2.70\times 10^{-24}$  J) is approximately two to three orders of magnitude smaller than theoretical expectation [8]. The DLP theory predicts a film thickness of the order of  $\sim 35$  nm at  $H=5$  mm for organic liquids on a Si wafer substrate, in contrast to our observations of only  $\sim 5$  nm for the film thickness at this height. We believe that the small value for the ‘‘effective’’ Hamaker constant  $W$  is due to the fact that AN probably only partially wets the Si wafer surface; Eq. (3) is strictly only correct under complete wetting conditions.
- [25] M. P. Nightingale and J. O. Indekeu, Phys. Rev. Lett. **54**, 1824 (1985); J. O. Indekeu, M. P. Nightingale, and W. V. Wang, Phys. Rev. B **34**, 330 (1986); M. Krech, Phys. Rev. E **56**, 1642 (1997); Z. Borjan and P. J. Upton, Phys. Rev. Lett. **81**, 4911 (1998).
- [26] P. Debye and K. Kleboth, J. Chem. Phys. **42**, 3155 (1965); M. J. Cooper, *ibid.* **48**, 4272 (1968); Y. Yosida, Phys. Lett. A **65**, 161 (1978).
- [27] *Handbook of Chemistry and Physics*, 66th ed., edited by R. C. Weast, M. J. Astle, and W. H. Beyer (CRC, Boca Raton, 1985).